12th A-PCNDT 2006 – Asia-Pacific Conference on NDT, 5th – 10th Nov 2006, Auckland, New Zealand

INFLUENCE OF CURVATURE ILLUMINATION WAVEFRONT IN QUANTITATIVE SHEAROGRAPHY NDT MEASUREMENT

Wan Saffiey Wan Abdullah

Malaysian Institute for Nuclear Technology Research (MINT), Bangi,
43000 Kajang, Malaysia
Tel: 6-03-89250510 Email: wansaffiey@mint.gov.my

Abstract

The applications of shearography technique for NDT and material evaluation have been acknowledged by many industries. However, the application is mainly limited to qualitative measurement. Studies show that the major problem encountered in quantitative measurement using this technique is related to error associated in the measurement system and other geometrical factors. In this paper, the analysis of the shearography equipment for field applications of out-of-plane and in-plane analysis is presented and discussed. The optical phase analysis when considering the error associated with the curvature of beam illumination and the imaging angle in the measurement are also presented. It was observed that the errors due to the curvature illumination and the imaging angle are higher than ±10% at object distance of less than 100cm. The in-plane error is found more predominantly compared to out-of-plane error. The theoretical error functions for both in-plane and out-of-plane measurements are also presented.

1. Introduction

Current trend of NDT inspection is more on the use of equipment that can provide real time, non-contact, non-invasive, full field, accurate and fast measurement time with quantitative data. The electronic speckle pattern shearing interferometry (ESPSI) or shearography is one of the technique that could full fill the above requirements, this method has been widely accepted in industrial applications particularly in aircraft and tire industries. In shearography data collection with digital format CCD camera provides an accuracy and safety of data storage, data can be further analyzed either in real time or using the stored data for quantitative values. It is well known that due to some limitation, most of commercial shearographic equipments use divergent or non-collimated illumination with assume the effect of beam curvature to the measurement value is very small and negligible.

The use of shearography in quality assurance and NDT, is involving out-of-plane displacement derivative (slope) ($\partial w/\partial x$ & $\partial w/\partial y$) or in-plane derivative measurements (strain, such as $\partial u/\partial x$), depending on the optical configuration, the nature and type of load imposed to the inspected object. Investigation has shown that the optical phase change can be measured within an accuracy of $\lambda/100$[1]. Error factors in the phase measurement accuracy such as due to the effect of environmental vibration, air turbulence, electronic noise, optical alignment and non-linearity of phase stepping device (PZT) are quantitatively been investigated [2,3]. However no attention has been made to correlate the effect with the nature of illumination wavefront and the size of illuminated area. This paper is to discuss on the error factor as functions of the properties of the illumination wavefront and the size of inspected area. The theoretical model of maximum phase change difference due to the former factors is also presented.

2. Theoretical Phase Analysis

Consider the wave fronts of the two speckle fields that sheared one relative to another. Let the wave front be represented by

$$U(x,y) = a\exp y\,(x,y) \tag{1}$$

and the sheared speckle field is given by

$$U(x+dx,y) = a\exp y\,(x+dx,y) \tag{2}$$

where $y\,(x,y)$ and $y\,(x+dx,y)$ represent the phase of light at points $A(x,y)$ and $A'(x+dx,y)$ on the image plane, and a is the light amplitude which is assumed equal for a neighbouring points. The total light field U_T measured on the image plane can be written as

$$U_T = U(x,y)+U(x+dx,y) \tag{3}$$

which give the light intensity I on the image plane as

$$I = U_T U_T^* = 2a^2(1+\cos\Delta) \tag{4}$$

where D is a random phase angle. The relative phase change of light scattered from point $A'(x+dx, y)$ to the light scattered from point $A(x, y)$ at any point on the object surface is given by

$$\Delta = y\,(x+dx,y) - y\,(x,y) \tag{5}$$

Work on the use of non-collimated illumination wavefront for a speckle pattern shearing interferometer with inclination angle [4] b as shown in Figure 1 depends on the illuminated object diameter and the distance from expanding lens to the object surface. The radius of wave front curvature R is the distance from the expansion lens to the center of inspected area of diameter D on the object surface, the value of inclination angle b can be calculated, and is given by [4]

$$b = \sin^{-1}\left[\frac{D}{2R}\right] \tag{6}$$

Another factor is due to the point on the illuminated area for which the phase is measured and represented by the imaging angle as [4, 5]

$$V = \tan^{-1}\left[\frac{D}{2L}\right] \tag{7}$$

where D is the inspected diameter and L is the distance from the center point of the inspected area to the CCD camera. Considering the function of inclination and imaging angles on the illuminated area of object surface, the theoretical phase function, Δ_x of the shearing interferometer for a non-collimated illumination wave front can be derived as [5]

$$\Delta_x = \frac{2p}{l}\left\{(1+\cos q)\frac{\partial w}{\partial x} + \sin q\,\frac{\partial u}{\partial x} + A\frac{\partial w}{\partial x} + B\frac{\partial u}{\partial x}\right\}dx \tag{8}$$

Where;

$$A = \tan\frac{b}{2}\sin q + \tan V\left\{\frac{\cos b + \tan\frac{\beta}{2}\sin q\cos(q-b)-1}{\sin(q-b)} - \sin q\right\} + \frac{1-\cos V}{\cos V}$$

$$B = \frac{1-\cos b - \tan\frac{b}{2}\sin q\cos(q-b)}{\sin(q-b)} - \sin V$$

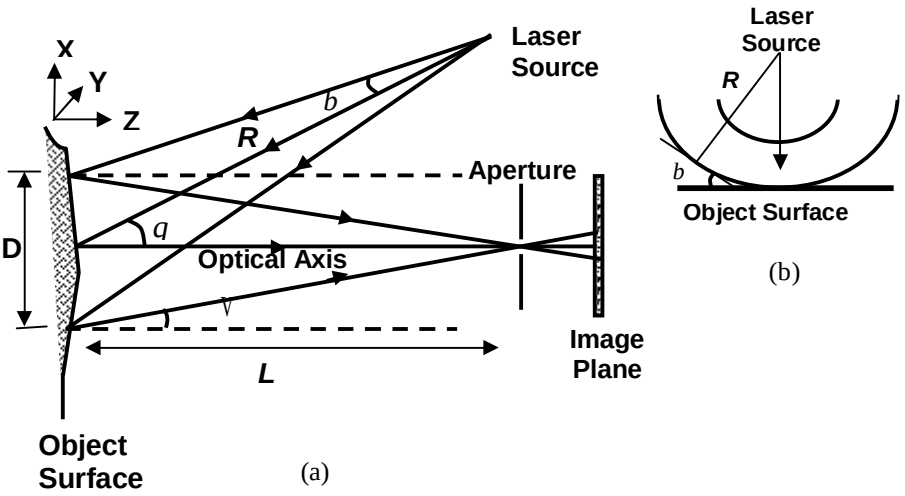

Figure 1: *(a) Schematic representative of the optical path length on the inspected object surface, (b) Inclination of the curvature illumination wavefront on the object surface.*

Considering situation at a point lies on the optical axis, this condition provides the values of imaging angle V and inclination angle b are zero, hence; $A = 0$, $B = 0$. Therefore the optical phase functions of Equation 8 becomes

$$\Delta_o = \frac{2p}{l}\left\{(1+\cos q)\frac{\partial w}{\partial x} + \sin q\,\frac{\partial u}{\partial x}\right\}dx \quad (9)$$

From Equation 8 of divergence illumination and Equation 9 for collimated illumination, the relative phase change difference is clearly a function of the nature of illumination wavefront and the geometrical factors. The maximum phase change difference, M_r of divergence and collimated illumination can be written as

$$M_r = \frac{\Delta_x - \Delta_{cx}}{\Delta_{cx}} = \frac{\tan\frac{b}{2}\sin q\,\frac{\partial w}{\partial x} + \tan V\left\{\frac{\cos b + \tan\frac{b}{2}\sin q\cos(q-b)-1}{\sin(q-b)}\right\}\frac{\partial w}{\partial x} + \left\{\frac{1-\cos b - \tan\frac{b}{2}\sin q\cos(q-b)}{\sin(q-b)}\right\}\frac{\partial u}{\partial x}}{(1+\cos q)\frac{\partial w}{\partial x} + \sin q\,\frac{\partial u}{\partial x} - \sin V\sin q\,\frac{\partial w}{\partial x} - \tan V\sin q\,\frac{\partial w}{\partial x} + \left\{\frac{1-\cos V}{\cos V}\right\}\frac{\partial w}{\partial x}} \quad (11)$$

The above equation is similar for collimated illumination only at single point lies on the center of optical axis. However at any point other than on the optical axis, the imaging angle $V \neq 0$ and $b = 0$, hence Equation 8 becomes

$$\Delta_{cx} = \frac{2p}{l}\left\{(1+\cos q)\frac{\partial w}{\partial x} + \sin q\,\frac{\partial u}{\partial x} - \sin V\,\frac{\partial u}{\partial x}\right\}dx$$

$$-\frac{2p}{l}\left\{\tan V\sin q\,\frac{\partial w}{\partial x} + \left(\frac{1-\cos V}{\cos V}\right)\frac{\partial w}{\partial x}\right\}dx \quad (10)$$

For in-plane analysis, the pure in-plane phase difference of the collimated wavefront at the edge of illuminated area with imaging angle V, can be written as

$$\Delta_{cx} = \frac{2p}{l}(\sin q - \sin V)\frac{\partial u}{\partial x}dx \quad (12)$$

Earlier investigation showed that the relat plane phase change difference profile was discontinues and not symmetric in the positive and negative illumination angles[5]. For simplicity of the theoretical phase change difference analysis and without changing any value, it is necessary to expand Equation 12 into meaningful forms, which can be written as

$$\Delta_{x2} = \frac{2p}{l}\left\{\frac{1}{2}(\sin q - \sin V)\frac{\partial u}{\partial x}\right\}dx$$

$$+\frac{2p}{l}\left\{\frac{\tan\frac{b}{2}\sin V\sin(q-b)[2\sin q - \sin V]}{\sin(q-b)}\right\}\frac{\partial u}{\partial x}$$

$$\Delta_{cx} = \Delta_{cx1} + \Delta_{cx2} = \frac{2pdx}{l}\left\{\frac{1}{2}(\sin q - \sin V)\frac{\partial u}{\partial x}\right\}$$

$$+ \frac{2pdx}{l}\left\{\frac{1}{2}(\sin q - \sin V)\frac{\partial u}{\partial x}\right\} \qquad (13)$$

where;

$$\Delta_{cx1} = \Delta_{cx2} = \frac{2pdx}{l}\left\{\frac{1}{2}(\sin q - \sin V)\frac{\partial u}{\partial x}\right\}$$

It should be emphasized that Equations 12 was generated assuming the use of an in-plane ESPSI interferometer with single illumination, and the error terms associated with other systematic or random uncertainty sources is not taken into account.

Consider an object placed along the *xz*-plane, which is in the same plane as the camera axis and behaving predominantly with in-plane motion. This condition could provide a value of $\partial w/\partial x$ approximately zero and can be considered as being negligible. Pure in-plane phase contribution at the edge of illuminated area should be written as

$$\Delta_x = \frac{2p}{l}\left\{(\sin q - \sin V)\frac{\partial u}{\partial x} + \left[\frac{1-\cos b - \tan\frac{b}{2}\sin q\cos(q-b)}{\sin(q-b)}\right]\frac{\partial u}{\partial x}\right\}dx \qquad (14)$$

Further expanding of Equation 14 and without changing any values, the phase equation can be written as

$$\Delta_x = \Delta_{x1} + \Delta_{x2} \qquad (15)$$

Where;

$$\Delta_{x1} = \frac{2p}{l}\left\{\frac{1}{2}(\sin q - \sin V)\frac{\partial u}{\partial x} + \tan\frac{b}{2}(\sin q - \sin V)^2\frac{\partial u}{\partial x}\right\}dx$$

Referring to Equations 13 and 15, and considering only the relative phase difference of the first part of these equations, the relative maximum phase change difference of divergence and collimated wavefront can be expressed as

Referring to Equations 13 and 15, and considering the relative phase difference of the second part of these equations, the relative maximum phase change difference of divergence and collimated wavefront can be expressed as

$$M_{r1} = \frac{\Delta_{x1} - \Delta_{cx1}}{\Delta_{cx1}} = 2\tan\frac{b}{2}(\sin q - \sin V) \qquad (16)$$

Referring to Equations 13 and 15, and considering tangent function as a positive constant, it can be seen that the phase value of $\Delta_{x1} \geq \Delta_{cx1}$ for all illumination angles. This explanation indicates that the phase difference function due to the second function of Equation 15 is in the positive quadrant, this give the value

$$M_{r2} = \frac{\Delta_{x2} - \Delta_{cx2}}{\Delta_{cx2}} \qquad (17)$$

$$= \frac{2\left\{1 - \cos b - \tan\frac{b}{2}\sin q\left[\cos(q-b) + \sin q\sin(q-b)\right]\right\}}{(\sin q - \sin V)\sin(q-b)}$$

$$+ \frac{2\left\{\tan\frac{b}{2}\sin V\sin(q-b)\left[2\sin q - \sin V\right]\right\}}{(\sin q - \sin V)\sin(q-b)}$$

of M_{r1} in Equation 16 is in the positive quadrant, $0 < q \leq \pi/2$ and the value of M_{r2} in Equation 17 is in the negative quadrant, $0 \geq q > -\pi/2$. It should be emphasized that the theoretical phase formulated was based on the initial experimental results using predominately plain strain test object.

3. Experimental Validation and Results

3.1 The maximum phase change different versus object distance of out-of-plane analysis

The change of wavefront curvature, on the structure and quality of the ESPSI correlation fringes, with respect to changing object distance, is one of the main interests of this study. Experiments using the cantilever beam from mild steel of 100mm length, 3mm thickness, and 30mm width, clamped rigidly at one end. The free end of the beam rest against a steel ball bearing providing point contact with a differential micrometer. The load applied for the cantilever beam deformation in these experiments used a Mitutoyo differential micrometer with an accuracy of ±1.5μm (manufacturer quoted). The cantilever beam provided well understood behaviour when subjected to load at the free end. Measurements derived for various degrees of divergent illumination were compared with measurements using collimated illumination. In order to change the curvature of the illumination wavefront, the distance from the object surface to the expanding lens was varied from 400mm to 1000mm (increments of 200mm) at each illumination angle and the amount of horizontal shearing were fixed to 5mm and 15mm with load of 20μm (0.566N) and 10μm (0.283N) respectively. The aperture size $F^{\#}$ was set between 5.6 and 6.5 depending on the brightness of the object image. The illumination angles were fixed at 5°, 30°, 45° and 60° relative to the camera axis.

Figure 2 shows the relationship of the relative maximum phase change difference (%) as function of the inspected object distance to the expanding lens, and the shearing amount. For a given inspected area, the relative maximum phase change difference due to wavefront curvature is very significant at shorter object distance and reduces approximately by a power function as the object distance increases. Experimental results also shows that the magnitude of the relative maximum phase change difference is a function of the shearing amount, the maximum phase change difference increases as the shearing amount increases, and this is clearly demonstrated in Figure 2(a) and 2(b). The theoretical fitting represents an ideal maximum phase change difference trend due to the wavefront curvature function with the change of object distance. Results of the experiments indicate a clear correlation with the proposed analytical maximum phase change difference predictions derived in Equation 11.

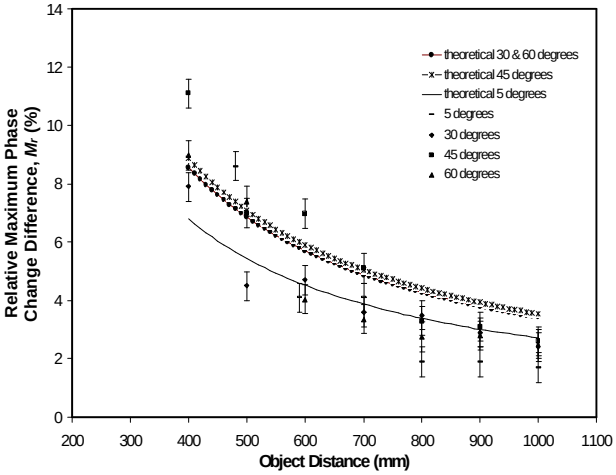

(a)

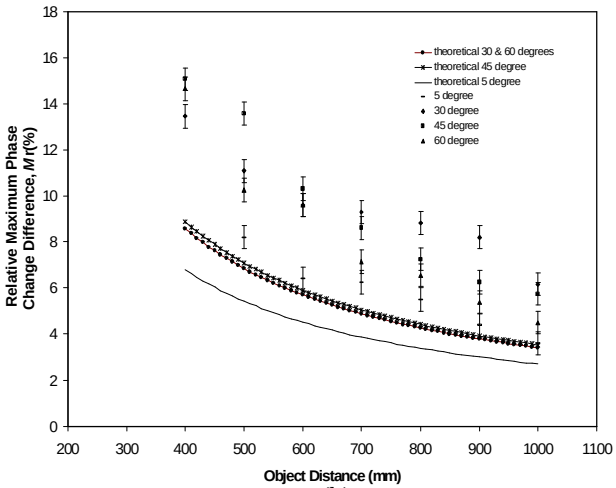

(b)

Figure 2: *Relative maximum phase change difference versus object distance for a different illumination angles, with a horizontal shears of (a) 5mm and (b) 15mm and illuminated area of 100mm x 30mm.*

3.2 The maximum phase change different versus object distance of in-plane analysis

In-plane maximum phase change difference propagation for which the beam lies horizontally with the change of object distance and fixed illumination direction was further investigated. The object consisted of commercial grade extruded aluminium alloy (HE30TB, E = 69GNm^{-2} and r = 2770kgm^{-3}). In order to produce predominantly IP motion, the object base and beam were fabricated as one solid piece. The dimensions of the object base is 50mm depth, 68mm width and 40mm height. The beam was machined from the solid block to a size of 140mm length, 20mm width and 20mm depth and left at the base center. The point load applied by the differential micrometer at 20mm from the beam end providing a 120mm length for measurement, which is the length from base to the load point. With these configuration the second bending moment of the object was calculated and the load required to produce a 1.0µm displacement at load point was 1.59N. The object illumination angles were chosen and fixed at four different angles of 45°, 60°, -45° and -60°. These angles are common and often used in the in-plane measurements. The load applied at positive illumination angles with vertical shearing of 5mm was 111.3N (70µm) and for 10mm shearing was 63.6N (40µm) respectively. At the negative illumination angles the load with 5mm shearing was 159N (100µm) and for 10mm shearing was 79.5N (50µm) respectively. The closest achievable distance from the expanding lens to the object surface was 200mm (the minimum distance in which the illumination on the object surface was set to be not less than 13.5% or 1/e^2 of the maximum illumination intensity). At a fixed illumination angle, a series of measurements was performed from the closest distance of 200mm to a distance of 1000mm with 100mm increments. The measurements of optical phase using a diverging illumination wavefront, was measured and compared with a similar analysis using an identical Michelson based shearing interferometer with collimated illumination (diameter of 135mm), without changing any of the other experimental parameters.

The relative maximum phase change difference propagation (%) with the change of inspected object distance to the expanding lens for different shearing amounts and a fixed illumination angle is shown in Figure 3. For a given inspected object dimension, the relative maximum phase change difference due to illumination wavefront curvature is very significant which exceeds 40% at shorter object distances and reduces approximately by a power function as the illumination curvature on the object surface decreases. Their magnitude is reversed when the illumination angle was changed to the negative sign. These trends are similar for derivative out-of-plane ESPSI. Experimental results also indicate that the magnitude of the relative maximum phase change difference is a function

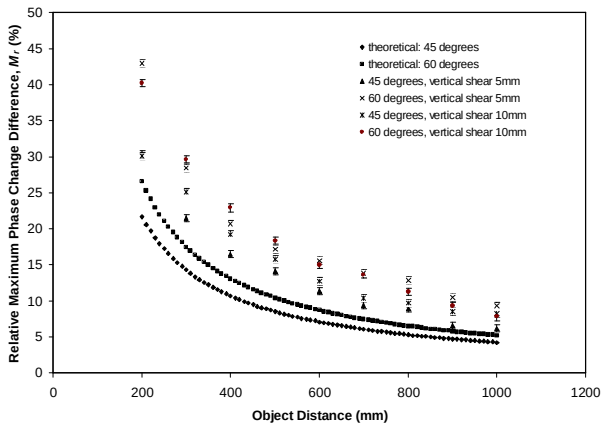

(a)

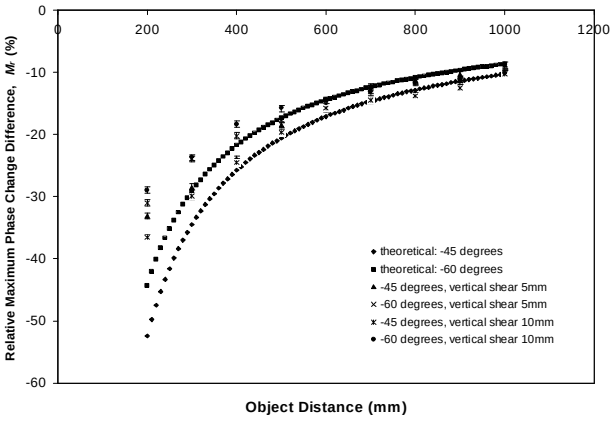

(b)

Figure 3: *The relation of relative maximum phase change difference with the change of object distance (illumination curvature) for different shearing amount, the free end of the beam at right side relative to the camera axis, (a) positive illumination angles at 45° and 60°, (b) negative illumination angles at -45° and -60°.*

of the shearing amount, which is slightly increased as the shearing amount increases. More importantly the maximum phase change difference function is dependent on the direction of illumination, the distance from the source to the object (the inclination angle, *b*) and the imaging angle (*V*). The theoretical fitting line (dotted line) represents the predicted maximum phase change difference trend due to the wavefront curvature function with the change of object distance. Results of the experiments as shown in Figure 3 is clearly correlated with the proposed theoretical maximum phase change difference derived in Equations 17 and 18. Its magnitude is slightly increased with the amount of the lateral shearing. Its trend follows the form of the theoretical fitting lines, but with increasing off-set as the amount of shearing increases. This phenomenon is in line with the theoretical analysis reported in the previous publications [6].

4. Conclusions

The use of non-collimated illumination in shearography NDT quantitative measurement can contributes a significant phase change difference which lead to error factor. The optical phase change difference associated with the divergence illumination wavefront analysis is theoretically derived and experimentally validated for both in-plane and out-of-plane deformation using two standard out-of-plane and in-plane cantilever beams. The phase change difference of divergence and collimated illuminations were found to vary significantly with the change of object to source distance, the illumination angle and the shearing amount. The magnitude of phase change variation can be worse than 10% for out-of-plane and 40% for in-plane deformation.

5. References

[1] Goodman, J.W., "Statistical properties of laser speckle pattern", Laser speckle and related phenomena (second edition), J.C. Dainty, Springer-Verlag Berlin, Germany, ISBN 0-387-13169-8, 1984.

[2] Archbold E., Burch J. M. and Ennos A. E., "Recording of in-plane surface displacement by double-exposure speckle photography", Opt. Acta 17(12) 883-898, 1970.

[3] Stetson K. A., "A review of speckle photography and interferometry", Opt. Eng. 14(5), 482-489, 1975.

[4] Wan Abdullah W S, Petzing J N & Tyrer J R.," Wavefront divergence: a source of error in quantified speckle shearing data", Journal of Modern Optics 48(5), 737-772, 2001.

[5] Wan Abdullah W. S., "Analysis of error functions in speckle shearing interferometry", A doctorial thesis, Loughborough University, United Kingdom, 2001.

[6] Steinchen W., Yang L., Mäckel G., Mäckel P., and Vössing F., "Digital-shearography for strain measurement –an analysis of the measuring error", SPIE 3479, 235-246, 1998.